AR-NE1A/ 2014G577

Magnetic structure of Fe_3O_4 (111) surfaces

Kanta Asakawa[1],Taizo Kawauchi[1], Xiao Wei Zhang[2], and Katsuyuki Fukutani[1]
[1]Institute of Industrial Science, University of Tokyo, Japan
[2]High Energy Accelerator Research Organization (KEK), Japan

Abstract: The magnetic structure of the Fe_3O_4(111) surface was investigated by conversion electron Mossbauer spectroscopy (CEMS) and nuclear resonant X-ray scattering (NRS). An $^{57}Fe_3O_4$ layer of about 1 nm was formed on a single-crystal Fe_3O_4(111) in an ultrahigh vacuum, and the magnetization at the surface was probed by CEMS and NRS. Both CEMS and NRS revealed resonance signals corresponding to the Fe A and B sites. From the analysis of the data, we discuss that the magnetization direction is near in-plane at the surface.

1 Introduction

Magnetite (Fe_3O_4) has attracted interest due to its fascinating characters such as catalytic activity [1,2] and predicted half-metallicity [3,4]. It also exhibits a metal-to-insulator transition at a transition temperature (T_v) of 120 K called the Verwey transition [5]. This is observed as a discontinuous drop in the electrical conductivity. In ambient conditions, Fe_3O_4 has the inverse-spinel cubic structure with space group $Fd^{-}3m$. Its unit cell contains 32 O atoms and 24 Fe atoms. The 24 Fe atoms consist of 8 tetrahedrally coordinated Fe(A) sites that are occupied by Fe^{3+} ions and 16 octahedral Fe(B) occupied by equal numbers of Fe^{2+} and Fe^{3+} ions [6-8]. Above 122 K, the electron hopping between Fe^{2+} and Fe^{3+} of B site gives rise to the electrical conductivity [9]. The decrease of electrical conductivity by the Verwey transition is explained by formation of charge ordering of B-site Fe^{2+} and Fe^{3+}. However, this mechanism is not experimentally confirmed despite intensive research in the last decades. There are, on the other hand, some reports claiming that the surface of Fe_3O_4 has an insulating character even at room temperature [3,9,10]. This might suggest that the surface Verwey transition occurs at a much higher temperature than 122 K [11,12]. Across the Verwey temperature, the crystallographic structure also changes from cubic ($T > T_v$) to monoclinic ($T < T_v$) [13,14]. Simultaneously, the magnetic easy axis changes from ⟨111⟩ to the monoclinic c axis[15-17]. In this study, the magnetization of the Fe_3O_4 (111) surface was investigated at room temperature using conversion electron Mossbauer spectroscopy (CEMS) and nuclear resonant X-ray scattering (NRS).

2 Experiment

Before CEMS and NRS experiments, an $^{57}Fe_3O_4$ layer was deposited on the surface in order to enhance the surface signal intensity. The deposition was performed in an ultrahigh vacuum (UHV) chamber with a base pressure of 1×10^{-10} mbar. The (111) surface of Fe_3O_4 single crystal was cleaned by Ar^+ sputtering, annealing at 1000 K and annealing in oxygen atmosphere of 5×10^{-6} mbar at 1000 K [18]. After cleaning, 1 nm of $^{57}Fe_3O_4$ epitaxial layer was grown by depositing ^{57}Fe in an oxygen atmosphere with a partial pressure of 8×10^{-6} mbar. The evaporation rate was approximately 0.2 nm/min and the sample temperature was kept at 550 K. After deposition, the sample was annealed in UHV at 800 K for 10 min [19]. The surface crystallinity was checked by reflection high-energy electron diffraction (RHEED) before and after deposition. NRS experiments were performed at the NE1 beam line of the accumulation ring (AR) of High Energy Accelerator Research Organization (KEK). The linearly polarized SR beam with an energy of 14.4 keV and energy width of 6.5 meV irradiated the sample with its electric polarization parallel to the surface. The reflected beam was detected by avalanche photodiodes (APD) set in the specular reflection direction [20]. During the experiment, the sample was kept at room temperature in a UHV chamber with a base pressure of 8×10^{-10} mbar. After installing the sample, NRS spectra were taken in six incident directions in order to estimate the in-plane magnetic anisotropy. After observing the azimuthal-angle dependence, the sample was cleaned by Ar+ sputtering, annealing at 1000 K and annealing in an oxygen atmosphere of 5×10^{-6} mbar at 1000 K. Finally, the NRS spectrum of the clean surface was observed with an incident angle parallel to the [1-10] axis. After the NRS experiments, the CEMS spectrum was observed in air at room temperature using a ^{57}Co source with the incidence angle parallel to the surface normal. A sample with natural abundance of ^{57}Fe was also used for comparison

3 Results and Discussion

Figure 1(a) and (b) shows the CEMS of natural and ^{57}Fe-enriched samples. The incident direction was parallel to the [111] axis. The six lines correspond to the $\Delta M = 0;\pm1$ excitations between the ground and excited states. The experimental data also shows two sites with different Zeeman splits. These sites correspond to the Fe(A) and Fe(B) sites [21]. The estimated internal magnetic fields were 48.6 and 45.5 T for the Fe(A) and Fe(B) sites, respectively. Also, the line intensity ratios were significantly different from that of the non-magnetized powder sample shown in figure 1(c). This is due to the magnetic anisotropy specific to the (111) surface. The averaged angle θ formed by the surface magnetization axis and the incident γ-ray direction was calculated using equations (1)-(3) [22]. For the ^{57}Fe-enriched sample, the angles were 104□ (A-site) and 101□ (B-site). For the

natural sample, θ was 110□(Asite) and and 106□(B-site). These values are close to the angle formed by four ⟨111⟩ axes, which means that only the in-plane ($[1\bar{1}\bar{1}]$, $[\bar{1}1\bar{1}]$ and $[\bar{1}\bar{1}1]$) magnetization axes are dominant on the (111) surface. The decrease in the angle after deposition might indicate that the magnetization is tilted even more parallel to the surface at the near-surface region.

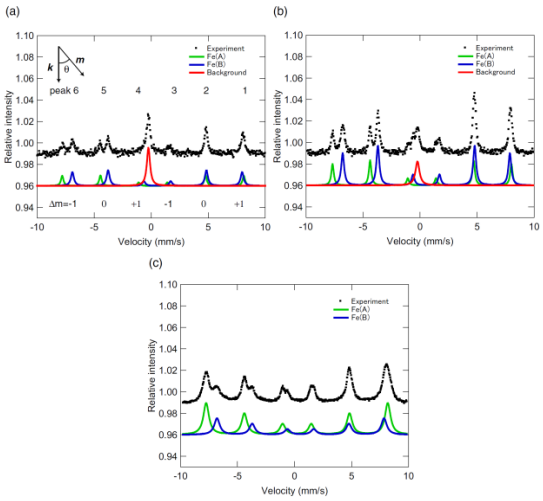

FIG. 1: Conversion electron Mossbauer spectrum (CEMS) of (a) natural Fe_3O_4 (111) surface, (b) 1 nm $^{57}Fe_3O_4$ on Fe_3O_4 (111) surface and (c) powder Fe_3O_4. The lines show the spectral components deduced from the ftting result. The background signal represented by the red line is derived from the sample holder.

$$W_1 = W_6 = 3(1 + \cos 2\ \theta\ )=2 \quad (1)$$
$$W_3 = W_4 = (1 + \cos 2\ \theta\ )=2 \quad (2)$$
$$W_2 = W_5 = 2 \sin 2\ \theta \quad (3)$$
W_{1-6} : relative line intensities

Figure 3(a) and (b) shows the time spectra of nuclear resonant X-ray and the corresponding frequency spectra for air-exposed surface taken at various azimuthal angles. The relationship between the frequency component and the magnetization axis is shown in figure 2. The intensities of the peaks at 170 and 182 MHz reflect the magnetization parallel to the electric field of the incident X-ray [23-25]. The intensities of the peaks at 170 and 182 MHz have weak dependence on the azimuthal angle, which suggests that the domains magnetized along three in-plane magnetization axes ($[1\bar{1}\bar{1}]$, $[\bar{1}1\bar{1}]$ and $[\bar{1}\bar{1}1]$) are equally dominant on the surface. Figure 4 shows the time spectrum taken after the cleaning procedure with an incident direction of $[10\bar{1}]$. The solid curve shows a fitting result. The fitting function is written as

$$I(t) = \sum_{\mu} i_{\mu}(t)$$

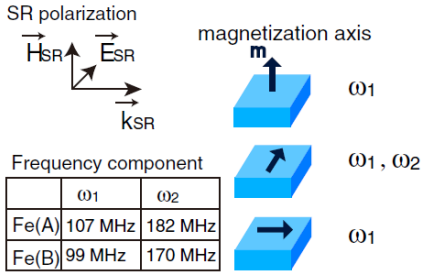

FIG. 2: Relation of the magnetization direction (**m**) with SR polarization and quantum-beat frequencies.

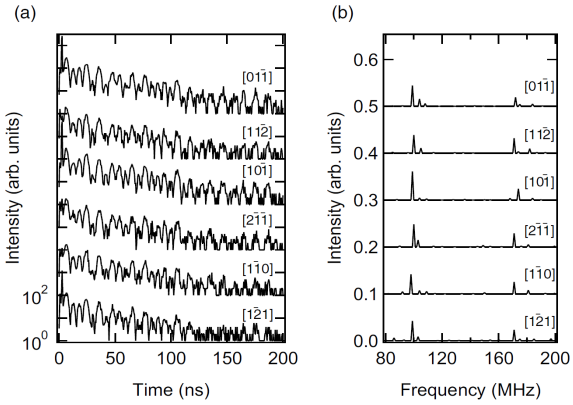

FIG. 3: Time spectra of nuclear resonant X-ray (a) and corresponding frequency spectra (b) observed at

$$i_{\mu}(t) = \left\{ \left| \left[\sum_{s} W_{s,\mu} \tilde{f}_{s,\mu}(t) \right]_{11} \right|^2 + \left| \left[\sum_{s} W_{s,\mu} \tilde{f}_{s,\mu}(t) \right]_{12} \right|^2 \right\} e^{-t/\tau_0}$$

s : Fe sites (Fe(A),Fe(B))

μ: Magnetization axis ($[111]$, $[1\bar{1}\bar{1}]$, $[\bar{1}1\bar{1}]$ and $[\bar{1}\bar{1}1]$)

Here, $\left[\tilde{f}_{s,\mu}(t)\right]_{ij}$ is the Fourier transformation of nuclear scattering length matrix element and τ_0 is the time constant. $W_{s,\mu}$ is the fitting parameter, which is proportional to the number of atoms of site s with magnetization axis μ. Also, from the absence of azimuthal-angle dependence of the time spectra, we assume

$$W_{s,[1\bar{1}\bar{1}]} = W_{s,[\bar{1}1\bar{1}]} = W_{s,[\bar{1}\bar{1}1]}$$

Table I shows the parameter $W_{s,\mu}$ obtained by fitting. This result indicates that the perpendicularly magnetized domain is absent in the near-surface region. Also, the Fe(B)/Fe(A) intensity ratio was 1.87, which is consistent with the bulk composition. These results also show that the perpendicularly magnetized domain is absent on Fe_3O_4 (111) surface. The most possible cause is the magnetostatic effect, which tend to rotate the magnetization parallel to the surface to form closure domains [26-27]. The decrease in angle θ after deposition

TABLE I: Parameter $W_{s,\mu}$ obtained by fitting the time spectrum of clean surface.

	$W_{perpendicular}$	$W_{in-plane}$
Fe(A)	0.00	1.13
Fe(B)	0.00	2.12

might indicate that magnetization even rotates towards the surface-parallel direction at the near-surface region. This may be due to the magnetostatic energy, which tend to rotate the magnetization to the surface-parallel direction. The size of this closure domain is several tens of micrometers [27], which is much larger than the probing depth of CEMS (about 100 nm).

4 Conclusion

We have studied the magnetization of the Fe_3O_4 (111) surface with CEMS and NRS. The results show that the perpendicularly magnetized domain is absent on the Fe_3O_4 (111) surface. The absence of azimuthal-angle dependence in NRS spectra indicates that domains magnetized along the other three magnetization axes ($[1\bar{1}\bar{1}]$, $[\bar{1}1\bar{1}]$ and $[\bar{1}\bar{1}1]$) exist equally. At the near-surface region, magnetization rotates from the original $\langle 111 \rangle$ axes to the surface-parallel direction. These can be attributed to the effect of magnetostatic energy.

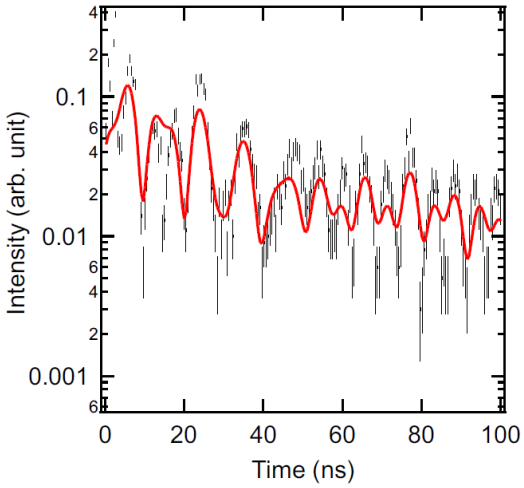

FIG. 4: Experimental data and the ftting curve of the NRS time spectra after cleaning procedure (Ar^+ sputtering, annealing and O_2 annealing).

References

[1] C. Martos, J. Dufour, and A. Ruiz, international journal of hydrogen energy 34, 4475 (2009).
[2] N. Mulakaluri et al., Physical Review Letters 103, 176102 (2009).
[3] G. Parkinson et al., Physical Review B 82, 125413 (2010).
[4] M. Kurahashi, X. Sun, and Y. Yamauchi, Physical Review B 81, 193402 (2010).
[5] E. Verwey, Nature 144, 327 (1939).
[6] S. Alvarado, M. Erbudak, and P. Munz, Physical Review B 14, (1976).
[7] Y. Dedkov et al., Physical Review B 70, 073405 (2004).
[8] Z. Zhang and S. Satpathy, Physical Review B 44, 13319 (1991).
[9] K. Jordan et al., Physical Review B 74, 085416 (2006).
[10] J.-H. Park et al., Phys. Rev. B 55, 12813 (1997).
[11] R. Wiesendanger et al., Science 255, 583 (1992).
[12] Z. Lodziana, Physical Review Letters 99, 206402 (2007).
[13] N. Otsuka and H. Sato, Journal of Solid State Chemistry 61, 212 (1986).
[14] Y. Miyamoto, S, and shin Chikazumi, Journal of the Physical Society of Japan 57, 2040 (1988).
[15] R. Aragon, Phys. Rev. B 46, 5328 (1992).
[16] Z. Kakol et al., Journal of Physics: Conference Series 303, 012106 (2011).
[17] K. Moloni, B. M. Moskowitz, and E. D. Dahlberg, 23, 2851 (1996).
[18] M. Paul et al., Physical Review B 76, 075412 (2007).
[19] N. Spiridis et al., Phys. Rev. B 85, 075436 (2012).
[20] T. Kawauchi et al., Physical Review B 84, 020415 (2011).
[21] R. Bauminger et al., Phys. Rev. 122, 1447 (1961).
[22] G. J. Long, Mossbauer spectroscopy applied to inorganic chemistry (Springer Science & Business Media,ADDRESS, 1984), Vol. 1.
[23] G. Smirnov, Hyperfine Interactions **123-124**, 31 (1999).
[24] G. V. Smirnov, Hyperfine Interactions **97-98**, 551 (1996).
[25] R. Rohlsberger, *Nuclear Condensed Matter Physics with Synchrotron Radiation: Basic Principles, Methodology and Applications* (Springer, ADDRESS, 2004), No. 208.
[26] S. Xu, D. J. Dunlop, and A. J. Newell, Journal of Geophysical Research: Solid Earth (1978{2012) **99**,9035 (1994).
[27] O. Ozdemir, S. Xu, and D. J. Dunlop, Journal of Geophysical Research: Solid Earth (1978{2012) **100**, 2193 (1995).

* fukutani@iis.u-tokyo.ac.jp